Vapor Phase Homogeneous Nucleation of Higher Alkanes: Dodecane, Hexadecane, and Octadecane. 2. Corresponding States and Scaling Law Analysis†

Mark Rusyniak and M. Samy El-Shall*

Department of Chemistry, Virginia Commonwealth University, Richmond, Virginia 23284-2006

Received: June 5, 2001

The results from corresponding states and scaled nucleation models indicate that the nucleation behavior of the normal alkanes follows a predictable trend. Systematic deviations from ideal fluid behavior can be correlated to physical properties, such as the increase in the entropy of vaporization and the increase in the excess surface entropy of the nucleating clusters. Hale's scaled nucleation model allows for the accurate prediction of nucleation threshold behavior for the alkanes. Experimental agreement with the model is maintained throughout the temperature range studied. The scaled model for the nucleation rate provides a better description of the experimental rates than the classical nucleation theory. The addition of extra terms to the classical expression of the free energy of cluster formation and the inclusion of the Fisher's droplet model term significantly compensate for the strong temperature dependence present in the flux prefactor of the classical rate equation. For accurate predictions of the nucleation rates, the proper inclusion of the configurational entropy term to the droplet free energy must be considered in a consistent manner.

I. Introduction

There is currently an enormous growth of interest in studying the vapor phase homogeneous nucleation for different classes of substances.[1] This interest is due in part to the need for comparing experimental data with predictions from different nucleation theories in order to develop an adequate quantitative theory. In addition, these measurements are important in determining the nucleating ability of different vapors and the conditions of their participation in the formation of ultrafine aerosols.[2]

Scaled models for homogeneous nucleation provide useful ways of correlating the experimental data for a series of different materials with their molecular properties.[3−18] In particular, scaling models deal with the correlation of critical supersaturations ($S_c(T)$), supersaturations required for the onset of nucleation at a rate of 1 drop/cm^3/s) and nucleation rates, $J(S,T)$, of wide classes of substances over wide ranges of experimental conditions using reduced (nondimensional) thermodynamic parameters. These correlations lead to identifying universal temperature dependencies, which complicate the extraction of general patterns from the nucleation data of individual substances.[3−18]

Systematic studies of homogeneous nucleation of different classes of compounds with a variety of molecular properties are desirable in order to test nucleation theories. Such studies provide insight into the role of different molecular properties in the nucleation process. This information is necessary in order to develop scaling laws for homogeneous nucleation, which are not dependent on any particular form of the theory. In this way, general patterns in nucleation behavior can be revealed that cannot be seen on the basis of a substance-by-substance comparison between experiment and theory. Toward this goal, we have examined the homogeneous nucleation of the nonpolar substances $SiCl_4$, $SnCl_4$, and $TiCl_4$.[19,20] In these systems, the experimental $S_c(T)$ agrees within a few percent with the predictions of classical nucleation theory (CNT). However, when the experimental results are compared among the series using a suitable dimensionless form, it becomes clear that $TiCl_4$ shows a different behavior compared to the other tetrachlorides CCl_4, $SiCl_4$, and $SnCl_4$. We have also studied the homogeneous nucleation of the highly polar substances, acetonitrile, benzonitrile, nitromethane and nitrobenzene where the dipole moments range from 3.5 to 4.4 D.[21−23] The experimental $S_c(T)$ of this series reveals significant disagreements with the predictions of the CNT.[21−23] The supersaturated vapors of these compounds are found to be more stable with respect to condensation than those of the weakly polar or nonpolar substances, which are well described by the CNT. In a recent study, we investigated the vapor phase homogeneous nucleation of a series of hydrogen bonding substances, namely ethylene glycol, propylene glycol, trimethylene glycol, and glycerol.[24] For these substances, it was found that at lower temperatures the measured $S_c(T)$ was lower than predicted by the CNT. Corresponding states analysis further revealed that glycerol exhibits nucleation behavior quite different from the other glycols: at the same reduced temperatures, glycerol required higher critical supersaturations.[24]

In this paper, we present the applications of scaled nucleation models to the nucleation data ($S_c(T)$ and $J(S,T)$) of the higher alkanes: dodecane, hexadecane, and octadecane. We also extend the scaling law analysis to all of the published data on the vapor phase homogeneous nucleation of the alkane series. The analyses are based on two scaled models for homogeneous nucleation. The first is the corresponding states approach developed by McGraw to predict the nucleation properties of different substances under constant reduced nucleation barrier height.[3] In the second approach, we employ the scaled model developed by Hale for the predictions of critical supersaturations and the temperature-dependent nucleation rates.[7,14]

† Part of the special issue "Howard Reiss Festschrift".

* To whom correspondence should be addressed.

10.1021/jp012118n CCC: $20.00
Published on Web 11/26/2001

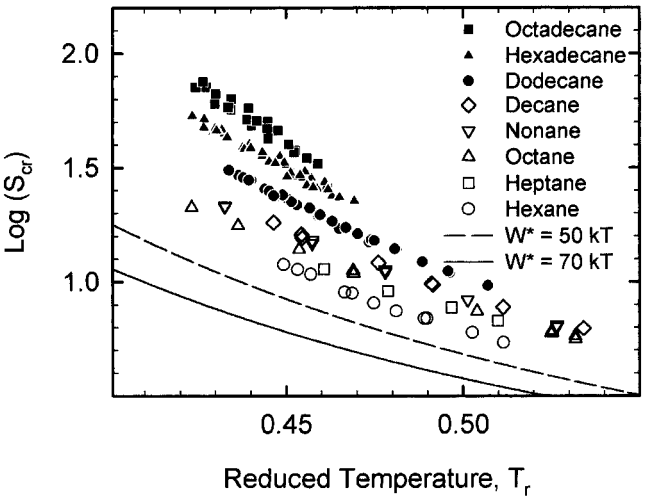

Figure 1. Critical supersaturation vs reduced temperature. The lower solid and upper dashed curves are for simple fluids and represent barrier heights of 70 and 50 kT, respectively.

II. Corresponding States Correlation

In this approach, the nucleation behavior of simple fluids serves as a reference point from which systematic deviations due to complex fluids can be revealed and easily associated with a particular molecular property. The free energy maximum of nucleation, W^*, (the barrier height) is expressed in the dimensionless form:

$$W^*/k_BT = 282.3G(T_r)(\log S)^{-2} \tag{1}$$

where

$$G(T_R) = \frac{T_R{}^{-3}(1 - T_r)^{11/3}}{[1 + 0.75(1 - T_r) + 1.75(1 - T_r)^{1/3}]^2} \tag{2}$$

k_B is Boltzmann's constant and $T_r = T/T_c$, where T_c is the critical temperature. Equation 1 is based on Guggenheim's empirical correlations of the surface tension and the number density of the heavier rare gases and therefore is a good approximation for the reduced barrier height of simple fluids.[25] For nucleation rates near unity ($J \sim 1$ cm^{-3} s^{-1}), W^* lies between $50k_BT$ and $70k_BT$. The dependence of supersaturation on T_r for simple fluids is shown in Figure 1 as solid and dashed curves for barrier heights of $70k_BT$ and $50k_BT$, respectively, along with the experimental S_c values for dodecane, hexadecane, and octadecane reported in paper 1.[26] Figure 1 also compares the S_c values of the lower molecular weight alkanes, hexane through decane, obtained from the literature.[27,28]

It is clear, from the results shown in Figure 1, that at a given reduced temperature the critical supersaturation increases with increasing chain length among the alkane series. Figure 1 also indicates that as the chain length increases the systematic departure from the nucleation behavior of simple fluids increases. This increased departure is a reflection of the increased complexity of the intermolecular interactions among the alkane molecules as the number of carbon atoms increases. The observed trend in log S_c vs T_r correlates well with the Pitzer acentric parameter ω of the alkanes as shown in Table 1. For example, *n*-hexane with a relatively small ω (0.299) has log S_c values slightly above the $50k_BT$ barrier height curve of simple fluids, whereas octadecane with a large ω of 0.812 has log S_c values significantly above the simple fluid curve. Because ω provides a measure of the excess entropy of vaporization over that of a simple fluid,[29] the systematic increase of log S_c with the chain length of the alkane reflects the increase in the entropy of vaporization among the alkane series.

TABLE 1: Scaling Law Parameter Ω and Acentric Parameter ω, for the *n*-alkane Series Calculated at a Reduced Temperature $T_r = 0.45$

compound	temp, K	Ω	ω
hexane	228.5	2.18	0.299
heptane	243.0	2.29	0.350
octane	256.0	2.37	0.397
nonane	267.0	2.44	0.443
decane	278.0	2.51	0.490
dodecane	288.6	2.60	0.573
hexadecane	318.7	2.89	0.737
octadecane	327.3	2.94	0.812

III. Scaled Nucleation Model

Hale developed a scaled nucleation model, valid at temperatures $T \ll T_c$, for qualitative analysis of homogeneous nucleation measurements and as a guide for systems with limited experimental parameters such as surface tension and vapor pressure data which are necessary to calculate the CNT predictions.[7,8,14] This scaled model has proven to be a powerful tool for correlating nucleation threshold behavior for diverse substances ranging from simple molecules[7,8] and nonpolar[9,19,20] and highly polar molecules[13,21−23] to metallic vapors and vapors of refractory materials.[10−12] For a nucleation rate of 1 cm^{-3} s^{-1}, the scaling law is expressed as[14]

$$\ln S_c = 0.53(\Omega[(T_c/T) - 1])^{3/2} \tag{3}$$

where Ω is the excess surface entropy per molecule in the cluster. The corresponding bulk liquid value of Ω can be approximated by the Eötvös constant,[30,31] K_e, which is defined as

$$k_BN_A{}^{2/3}\Omega \approx K_e = (M/\rho)^{2/3}\sigma/(T_c - T) \tag{4}$$

where M is the molecular weight, ρ is the liquid density, σ is the surface tension, and N_A is Avogadro's number. The Eötvös constant is roughly 2.1 for simple liquids and 1.5 for associated liquids. As shown by eq 4, the Eötvös constant is Ω times the constant $k_BN_A{}^{2/3} = 0.984$; therefore, Ω and K_e have nearly the same value. An alternative method for evaluating the excess surface entropy is to approximate $\sigma/(T_c - T)$ with the temperature dependence of the surface tension according to

$$\Omega = -\left[\frac{\partial\sigma}{\partial T}\right]/(k_B\tilde{n}^{2/3}) \tag{5}$$

where $\tilde{n}$ is the liquid number density.[13]

To investigate the effect of the parameter Ω on the predictive ability of the scaling law, we used eqs 4 and 5 to calculate Ω for the higher alkanes: dodecane, hexadecane, and octadecane at a midrange temperature of our data. Using these parameters, we calculated the critical supersaturation as a function of temperature using eq 3. The results are shown in Figure 2 where Ω calculated from eqs 4 and 5 are referred to as Ω_1 and Ω_2, respectively. It is clear that the Ω values calculated using eq 5 (3.35, 3.85, and 4.10 at 305, 325, and 330 K for dodecane, hexadecane, and octadecane, respectively) result in critical supersaturations in poor agreement with the experimental values across the entire temperature range. On the other hand, Ω values calculated from eq 4 (2.64, 2.87, and 2.97 at 305, 325, and 330 K for dodecane, hexadecane, and octadecane, respectively) result in remarkably good predictions of the critical supersaturations

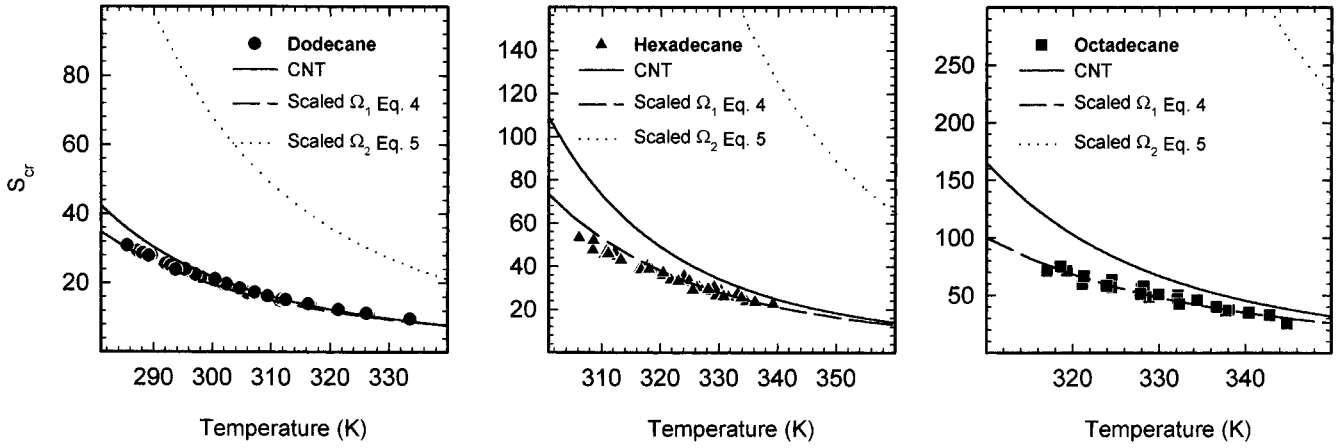

Figure 2. Critical supersaturation vs temperature as predicted from the scaling law using Ω calculated from eqs 4 and 5 for dodecane, hexadecane, and octadecane. The predictions of CNT are also shown for comparison.

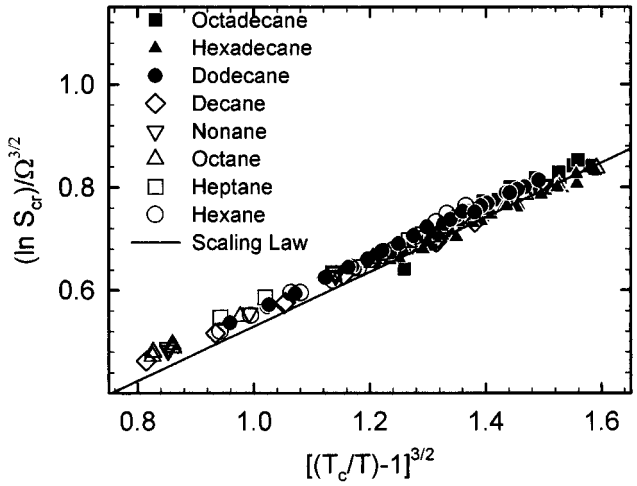

Figure 3. Scaled critical supersaturations for the *n*-alkane series. Solid line represents the prediction from the model.

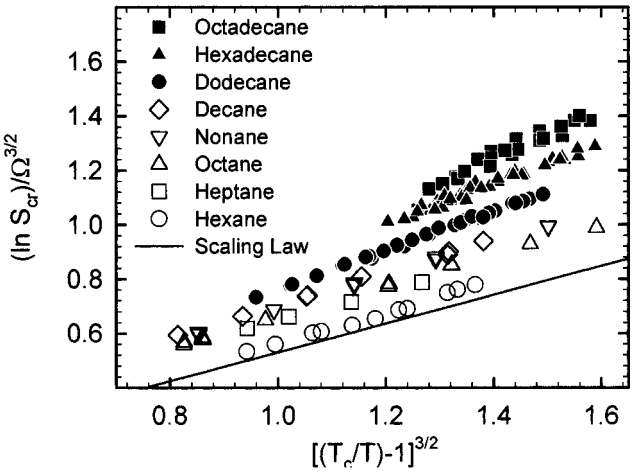

Figure 4. Scaled critical supersaturations for the *n*-alkane series using the scaling factor Ω = 2.12. Solid line represents the behavior of an ideal fluid.

as shown in Figure 2. Note that the agreement extends throughout the entire temperature range studied. This indicates that the use of the temperature dependence of the surface tension to approximate $\sigma/(T_c - T)$ can lead to substantial errors in the predictions of critical supersaturations by the scaled model. This result is consistent with the trend observed in the analysis of the nucleation data of glycols, where Ω calculated using eq 4 did a better job in the predictions of the critical supersaturations than the Ω calculated using eq 5.[24] A similar conclusion has been reached in the scaled model analysis of the condensation of metallic vapors.[12]

The results shown in Figure 2 also indicate that the Hale scaled model using the Ω parameter calculated based on the Eötvös constant does a better job of predicting the nucleation threshold of the higher alkanes than the CNT. Motivated by the excellent predictions of S_c for the higher alkanes, we extended the analysis of the scaled model to the full range of alkane data available in the literature.[27,28] The experimental data are plotted as $\ln S_c/\Omega^{3/2}$ vs $[(T_c/T) - 1]^{3/2}$ as shown in Figure 3, where the solid line in the graph represents the prediction of the model. The Ω values calculated using eq 4 are given in Table 1 at a constant reduced temperature of 0.45. It is clear that Hale's model allows for an accurate prediction of the threshold nucleation behavior of the normal alkane series. This is evident from the remarkable agreement between the experimental S_c and the predictions of the scaling law shown in Figure 3.

To correlate general patterns of nucleation behavior with molecular properties, one should use the ideal value of Ω of 2.12 corresponding to a simple fluid and examine the $S_c(T)$ among a series of structurally related molecules. The resulting pattern for the alkane series is shown in Figure 4 where the solid line serves as a convenient reference for the nucleation threshold of simple fluids. The systematic departure from this behavior is evident as the chain length increases among the alkane series as shown in Figure 4. It is interesting that both forms of the scaled law (McGraw's corresponding states approach and Hale's scaled model) result in the same systematic departure from the nucleation behavior of simple fluids as the size of the alkane molecules increases. This trend correlates with the increase in the entropy of vaporization as reflected in the Pitzer acentric parameter ω[29] and with the increase in the excess surface entropy of the nucleating clusters as reflected in the Eötvös parameter Ω.[30,31]

The measured supersaturations can be used to extract values for Ω using eq 3. Figure 5a exhibits plots of $\ln S_c$ vs $[(T_c/T) - 1]^{3/2}$ based on the experimental values of S_c. The linearity of the plots is evident and from the slopes of the lines, we calculate the Ω values of 2.59, 2.67, and 3.12 for dodecane, hexadecane, and octadecane, respectively. Obviously, these values are very close to the calculated ones using eq 4 because these values reproduce the experimental results. By rearranging eq 3, Hale's model can be used to estimate the critical temperature. Figure

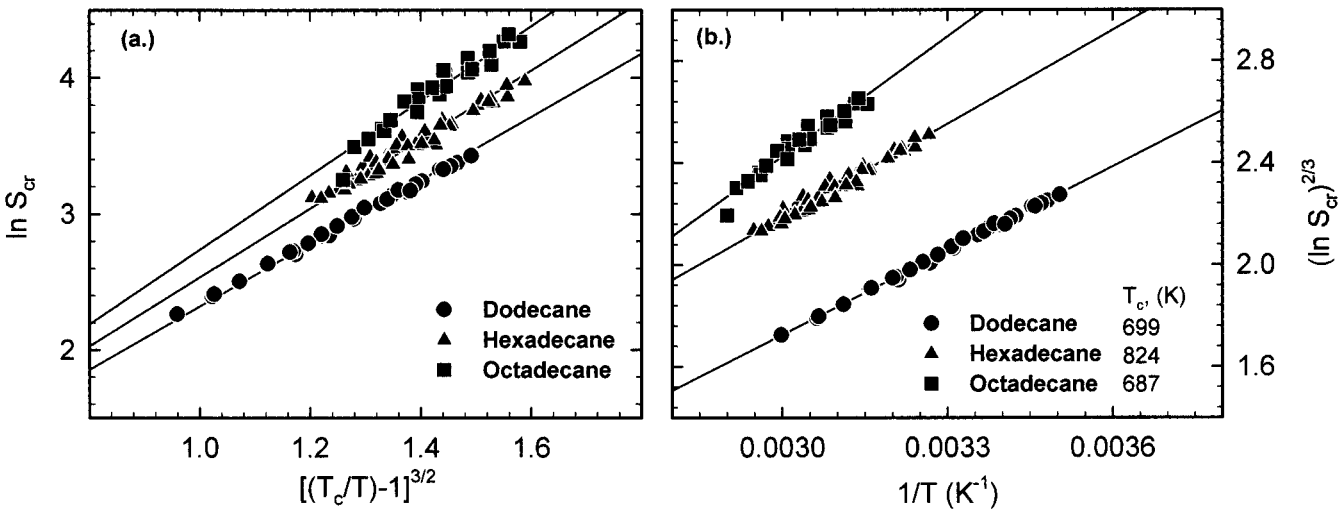

Figure 5. (a) ln S_c vs $[T_c/T - 1]^{3/2}$ for the studied compounds. Least-squares fit through the origin is used to determine the estimated values of Ω. (b) ln $S_c^{2/3}$ vs $1/T$, for the studied compounds. Least-squares fit is used to determine estimated values of the critical temperature.

5b shows $(\ln S_c)^{2/3}$ vs $1/T$, for the experimental data. In this case, the slope of the linear fit divided by the intercept gives the critical temperature. The estimated T_c from Figure 5b for dodecane, hexadecane, and octadecane are 699, 824, and 687 K, respectively. These estimates are higher than the literature values of T_c for dodecane, hexadecane, and octadecane by 6.4%, 13.9%, and 8.1%, respectively. However, It should be noted that the higher molecular weight alkanes decompose at temperatures in excess of around 650 K and that the literature values are themselves estimates.[32,33] The estimates that we obtained from nucleation data are in reasonable agreement with those cited.

IV. Scaled Model for the Nucleation Rate

Considering that the nucleation threshold conditions ($W^* \approx 50-70k_BT$) correspond to several orders of magnitude of uncertainty in the absolute nucleation rate, the scaled law prediction of S_c is not as a stringent test of the model as the prediction of the nucleation rate. Hale[14] extended the scaled model to the steady-state nucleation rate by deriving an expression for the scaled supersaturation ($\ln S/A^{3/2}$), where A is the coefficient of the surface term in the free energy of cluster formation $[W(n)/k_BT]$ according to the CNT

$$W(n)/k_BT = An^{2/3} - n \ln S \tag{6}$$

Using scaled surface tension through the parameter Ω, A can be expressed as

$$A = (36\pi)^{1/3}\Omega\left(\frac{T_c}{T} - 1\right) \tag{7}$$

The critical cluster size (n^*) and the scaled barrier height (W_s) are then given by

$$n^* = [2A/(3 \ln S)]^3 \tag{8}$$

$$W_s = \frac{16}{3}\pi\Omega^3\left[\frac{T_c}{T} - 1\right]^3/(\ln S)^2 \tag{9}$$

Hale[14] pointed out that the surface free energy for small clusters can be estimated by summing over free energy differences from $n' = 2$ to $n' = n$, which results in the expression

$$\sum\delta_{n'} \approx An^{2/3}\left[1 + \frac{1}{3n}\right] - \frac{4A}{3} \tag{10}$$

By using the expression in eq 10 to replace the $An^{2/3}$ term in the CNT energy of formation (eq 6) and including the "entropy cost" term $\tau \ln(n)$ introduced by Fisher[34] and later employed by Dillman and Meier,[35,36] the energy of cluster formation is now expressed as

$$W(n)/k_BT = An^{2/3}\left[1 + \frac{1}{3n}\right] - \frac{4A}{3} + \tau \ln n - (n-1)\ln S \tag{11}$$

where the term $(n - 1)$ is used so $W(1) = 0$.

Following the new expression for the free energy of formation, the critical size (n^*) is now given by

$$n^* = [2A/(3 \ln S)]^3 f(n^*) \tag{12}$$

where

$$f(n^*) = \left[1 - \frac{\tau}{n^* \ln S} + \frac{A}{9(n^{*4/3} \ln S)}\right]^{-3} \tag{13}$$

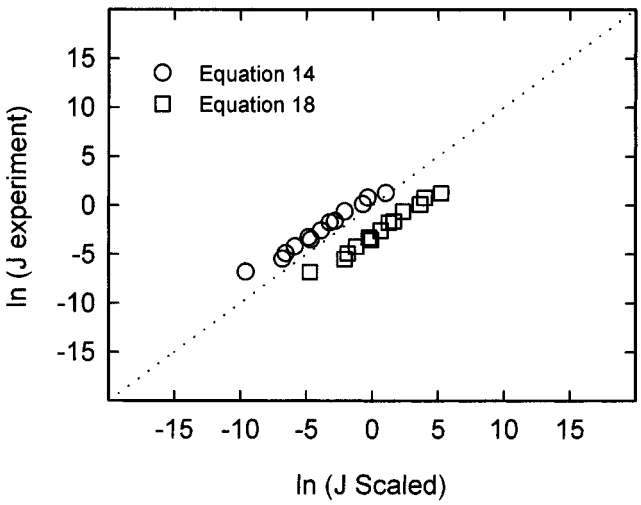

Figure 6. Comparison of the predictions of the scaled rate model using eqs 14 and 18 with the experimental rates of one isotherm for octadecane.

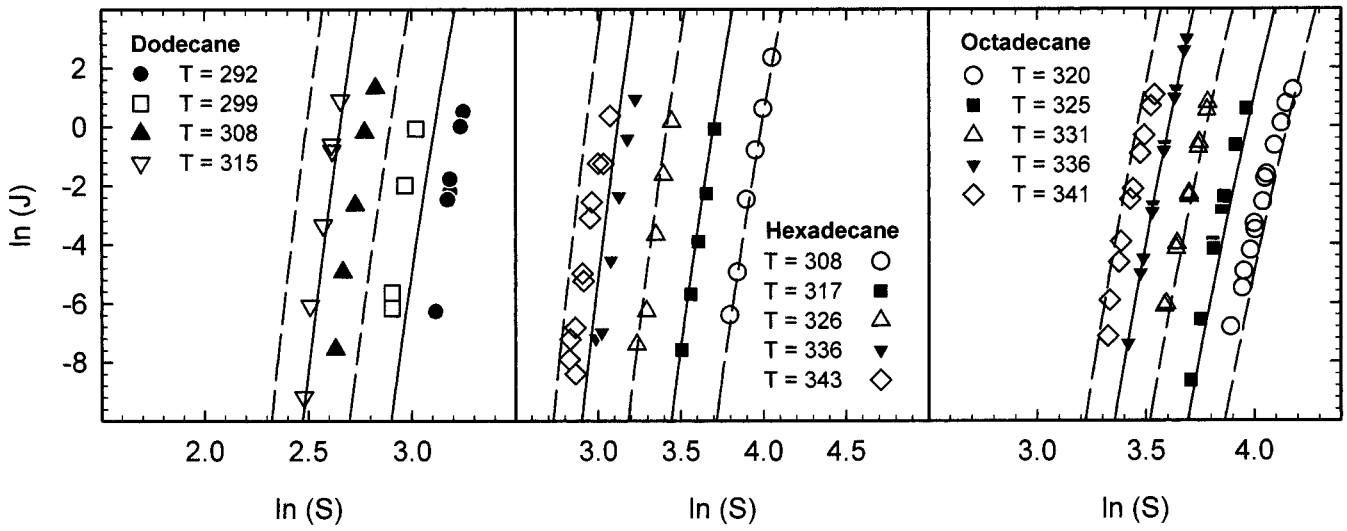

Figure 7. Isothermal nucleation rates compared with the predictions of the scaled rate model using eq 14 (lines represent the model results). See Figures 6−8 in paper 1 (ref 26) for comparison to the CNT.

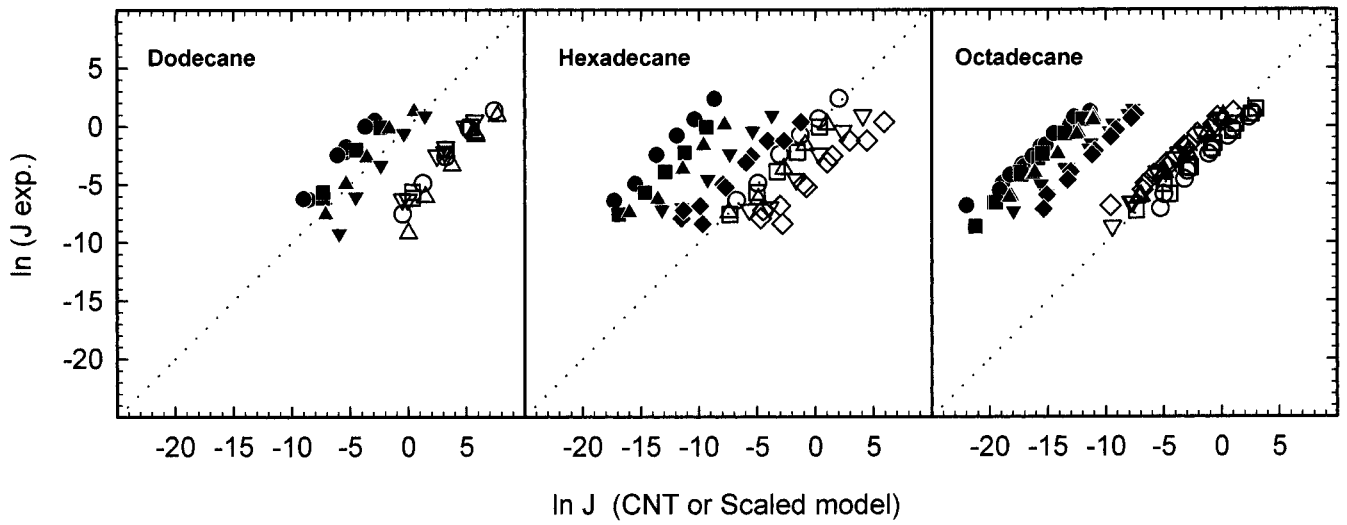

Figure 8. Experimental nucleation rates at different isotherms vs the predictions from the scaled model (open symbols) and the CNT (filled symbols).

Using the expression for (n^*), eq 12, Hale showed that the steady-state homogeneous nucleation rate (J) can be obtained from

$$\ln J = \ln J_0 + \frac{4}{3}A + \frac{3}{2}\tau - \tau \ln(n^*) - \frac{1}{2}An^{*-1/3} - \ln S - W_s f(n^*) \quad (14)$$

where

$$J_0 = J_c I [P/P_c]^2 S^2 \quad (15)$$

$$J_c = \frac{P_c^{\,2}}{hk_B T_c \Gamma_c}\left(\frac{\Gamma_c}{n_c}\right)^{2/3} \quad (16)$$

$$I = 2\left(\frac{\tilde{n}_c}{\tilde{n}}\right)^{2/3}\left[\Omega\left(\frac{T_c}{T} - 1\right)\right]^{1/2}\left(\frac{T_c}{T}\right)^{3/2} \quad (17)$$

In the above equations, J_0 is the kinetic prefactor for the homogeneous nucleation rate according to the CNT (including the Zeldovitch factor); $\Gamma_c = (2\pi m k_B T_c/h^2)^{3/2}$ is the inverse thermal wavelength cubed at T_c; and $\tilde{n}$, P, h, and k_B are the liquid number density, pressure, Planck constant, and Boltzmann constant. The subscript c denotes the critical-point quantities.

Equation 12 is solved iteratively to determine n^*. The value of τ can be determined using Riemann Zeta functions $\zeta(s) = \sum_{k=1}^{\infty} k^{-s}$ and the relation $\zeta(\tau)/\zeta(\tau - 1) = Z_c$ where Z_c is the critical compressibility ($Z_c = P_c/kT_c n_c$). Rational Chebyshev approximations are used to solve this relationship for τ. Using this procedure, the values of τ determined for dodecane, hexadecane and octadecane are 2.186, 2.177, and 2.154, respectively.

Hale[14] showed that an approximate form of eq 14 may be given by

$$\ln J \approx \ln \Gamma_c - W_s \quad (18)$$

The quantity $\ln \Gamma_c$ in eq 18 is found to be nearly constant (about 60 in cgs units) for most substances. For dodecane, hexadecane, and octadecane, the $\ln \Gamma_c$ values are calculated as 64.1, 64.7, and 64.9, respectively. We used eqs 14 and 18 to calculate the isothermal nucleation rates of dodecane, hexadecane, and octadecane and to compare the predictions of the scaled rate model with the experimental rates. An example from such a comparison is shown in Figure 6 for the nucleation rate

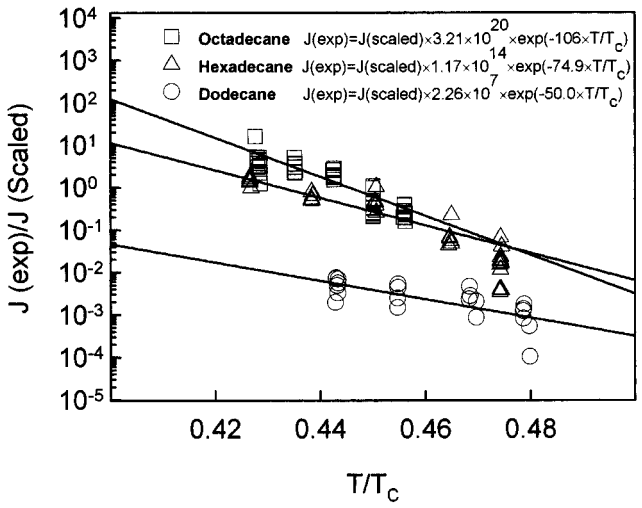

Figure 9. Scaled model prediction of nucleation rate fits to the experimental results showing the temperature dependent correction factors.

of octadecane. It is clear from the results presented in Figure 6 that eq 14 gives better agreement with the experimental data. The same trend was found in the analysis of the nucleation rate data of dodecane and hexadecane. However, it is interesting to note that despite the simplicity of eq 18 it provides reasonable predictions of both the temperature and supersaturation dependencies of the nucleation rate.

Figure 7 displays comparisons of the supersaturation dependence of the experimental rates with the calculated ones using eq 14 for dodecane, hexadecane, and octadecane. Figure 8 displays $\ln(J_{exp})$ versus $\ln(J_{scaled})$ for the three compounds at different nucleation temperatures. For comparison, the values of $\ln(J_{CNT})$ calculated from the CNT are also included in Figure 8. The results indicate that Hale's model predicts the correct dependence of the nucleation rate on supersaturation, similar to the CNT. However, the scaled model is superior to the CNT in predicting the temperature dependence in reasonable agreement with the experiment. This can be seen from Figure 8 where the scaled rates corresponding to different isotherms show less spread than the calculated rates using the CNT.

Figure 9 displays the ratios of ($\ln J_{exp}/\ln J_{scaled}$) as a function of T_r, along with the temperature correction factors for dodecane, hexadecane, and octadecane. In comparing the scaled model to the CNT for the higher alkanes (see Figure 8 of paper 1, ref 26), it is evident that the scaled model results in overall better temperature dependence than the CNT.

It is interesting to note that the success of the Hale's model is related to the introduction of the extra terms in the free energy of cluster formation which, through their temperature dependence, they tend to "compensate" for the strong temperature dependence present in the kinetic prefactor (as a result of the P^2 dependence) of the CNT rate equation. As suggested by Hale,[14] the added $^1/_3An^{-1/3}$ term to the surface free energy of the CNT expression of $W(n)/k_BT$, could be interpreted as an "effective" surface tension correction arising from the contribution of the small clusters to the total free energy. In fact, the combination of this term with the classical $An^{2/3}$ term produces an expression similar to the Tolman's correction to the curvature dependence of the surface tension.[24,38] One may also suspect that the inclusion of the configurational entropy term $\tau \ln(n)$ in the energy of cluster formation could have an important role in determining the level of agreement between the scaled model as described by eq 14 and the experimental data. Unfortunately, the $\tau \ln(n)$ term, which is present at the critical point in Fisher's droplet model,[34] remains a term not well understood nor substantiated in nucleation models for temperatures far below the critical point. At the same time, it appears that by considering the $\tau \ln(n)$ and the $^1/_3An^{-1/3}$ terms the temperature dependence of the CNT can be brought to close agreement with the experimental data. These problems, like that of the "replacement free energy",[39,40] can be effectively addressed by rigorous statistical mechanical molecular treatments such as the molecular theory of nucleation[39,40] or density functional theory.[41,42]

V. Conclusions

The results from corresponding states and scaled nucleation models indicate that the nucleation behavior of the normal alkanes follow a predictable trend. Systematic deviations from ideal fluid behavior can be correlated to physical properties, such as the increase in the entropy of vaporization as reflected in the Pitzer acentric parameter ω and with the increase in the excess surface entropy of the nucleating clusters as reflected in the Eötvös parameter Ω. Hale's scaled nucleation model allows for the accurate prediction of nucleation threshold behavior for the alkanes. Experimental agreement with the model is maintained throughout the temperature range studied. The scaled model for the nucleation rate provides better description of the experimental rates than the classical nucleation theory. The addition of the extra terms arising from the summing discretely over small cluster free energy differences and the inclusion of the Fisher's droplet model term significantly compensate for the strong temperature dependence present in the flux prefactor of the CNT rate equation. Rigorous statistical mechanical molecular treatments should be able to identify the correct descriptions of the kinetics and thermodynamics of the nucleation process that will quantitatively agree with the experimental data.

Acknowledgment is made to NASA Microgravity Materials Science Program (NAG8-1484) for the support of this research.

References and Notes

(1) Heist, R. H.; He, H. *J. Phys. Chem. Ref. Data* **1995**, *23*, 781.
(2) *Nucleation and Atmospheric Aerosols 2000*; Hale, B. N., Kulmala, M., Eds.; American Institute of Physics: Woodbury, NY, 2000.
(3) McGraw, R. *J. Chem. Phys.* **1981**, *75*, 5514.
(4) Garnier, J. P.; Mirabel, P.; Rabeony, H. *J. Chem. Phys.* **1983**, *79*, 2097.
(5) Rasmussen, D. H.; Appleby, M. R.; Leedom, G. L.; Babu, S. V. *J. Cryst. Growth* **1983**, *64*, 229.
(6) Rasmussen, D. H.; Babu, S. V. *Chem. Phys. Lett*. **1984**, *108*, 449.
(7) Hale, B. N. *Phys. Rev. A* **1986**, *33*, 4156.
(8) Hale, B. N. In *Lecture Notes in Physics*. *Scaled Models for Nucleation*; Wagner, P. E., Vali G., Eds.; Springer: New York, 1988; Vol. 309, pp 323−349.
(9) El-Shall, M. S. *J. Phys. Chem.* **1989**, *93*, 8253.
(10) Hale, B. N.; Kemper, P.; Nuth, J. A., III. *J. Chem. Phys*. **1989**, *91*, 4314.
(11) Nuth, J. A., III.; Ferguson, F. T. In *Nucleation and Crystallization in Liquids and Glasses*; Weinberg, M. C., Ed.; American Ceramic Society: Westerville, OH, 1993; Vol. 30, p 23.
(12) Martinez, D. M.; Ferguson, F. T.; Heist, R. H.; Nuth, J. A., III. *J. Chem. Phys.* **2001**, *115*, 310.
(13) Hale, B. N.; Kelly, B. *Chem. Phys. Lett.* **1992**, *189*, 100.
(14) Hale, B. N. *Metall. Trans. A* **1992**, *23*, 1863.
(15) McGraw, R.; Laaksonen, A. *Phys. Rev. Lett.* **1995**, *76*, 2754.
(16) Talanquer, V. *J. Chem. Phys.* **1997**, *106*, 9957.
(17) Koga, K.; Zeng, X. C. *J. Chem. Phys.* **1998**, *110*, 3466.
(18) Hale, N. B.; Wilemski, G. *Chem. Phys. Lett.* **1999**, *305*, 263.
(19) El-Shall, M. S. *Chem. Phys. Lett.* **1988**, *143*, 381.
(20) El-Shall, M. S. *J. Chem. Phys.* **1989**, *90*, 6533.
(21) Wright, D.; Caldwell, R.; El-Shall, M. S. *Chem. Phys. Lett.* **1991**, *176*, 46.
(22) Wright, D.; El-Shall, M. S. *Chem. Phys. Lett.* **1992**, *189*, 103.

(23) Wright, D.; Caldwell, R.; Moxely, C.; El-Shall, M. S. *J. Chem. Phys.* **1993**, *98*, 3356.
(24) Kane, D.; El-Shall, M. S. *J. Chem. Phys.* **1996**, *105*, 7617.
(25) Guggenheim, E. A. *J. Chem. Phys*. **1945**, *13*, 253.
(26) Rusyniak, M.; Abdelsayed, V.; Campbell, J.; El-Shall, M. S. *J. Phys. Chem. B* **2001**, *105*, 11866.
(27) Katz, J. L. *J. Chem. Phys.* **1970**, *52*, 4733.
(28) Rudek, M. M.; Fisk, J. A.; Chakarov, V. M.; Katz, J. L. *J. Chem. Phys.* **1996**, *105*, 4707.
(29) Pitzer, K. S.; Lippmann, D. Z.; Curl, R. F., Jr.; Huggins, C. M.; Petersen, D. E. *J. Am. Chem. Soc.* **1955**, *77*, 3433.
(30) Bondi, A. In *Physical Chemistry: Enriching Topics from Colloid and Surface Science*; van Olphen, H., Mysels, K. J., Eds.; Theorex: La Jolla, CA, 1975; pp 93−125.
(31) Moelwyn-Hughes, E. A. *Physical Chemistry*; Pergamon Press: Oxford 1965; p 930.
(32) Vega, C.; Macdowell, L. G. *Mol. Phys.* **1996**, *88*, 1575.
(33) Smit, B.; Karaborni, S.; Siepmann, J. I. *J. Chem. Phys.* **1995**, *102*, 2126.
(34) Fisher, M. E. *Physics* **1967**, *3*, 255.
(35) Dillmann, A.; Meier, G. E. A. *Chem. Phys. Lett.* **1989**, *160*, 71.
(36) Dillmann, A.; Meier, G. E. A. *J. Chem. Phys.* **1991**, *94*, 3872.
(37) Cody, W. J.; Hillstrom, K. E.; Thacher, H. C., Jr. *Math. Comput.* **1971**, *25*, 537.
(38) Tolman, R. C. *J. Chem. Phys.* **1949**, *17*, 118.
(39) Reiss, H.; Kegel, W. K.; Katz, J. L. *J. Phys. Chem. A* **1998**, *102*, 8548.
(40) Reiss, H. *Nucleation and Atmospheric Aerosols 2000*; American Institute of Physics: Woodbury, NY, 2000; p 181−196.
(41) Zeng, X. C.; Oxtoby, D. W. *J. Chem. Phys.* **1991**, *94*, 4472.
(42) Talenquer, B.; Oxtoby, D. W. *J. Chem. Phys.* **1994**, *100*, 5190.